

# Synthesis of isobenzofuran derivatives from renewable 2-carene over halloysite nanotubes

A.Yu. Sidorenko<sup>a,b,\*</sup>, A.V. Kravtsova<sup>a</sup>, P. Mäki-Arvela<sup>b</sup>, A. Aho<sup>b</sup>, T. Sandberg<sup>b</sup>, I.V. Il'ina<sup>c</sup>, N.S. Li-Zhulanov<sup>c,d</sup>, D.V. Korchagina<sup>c</sup>, K.P. Volcho<sup>c,d</sup>, N.F. Salakhutdinov<sup>c,d</sup>, D.Yu. Murzin<sup>b,\*\*</sup>, V.E. Agabekov<sup>a</sup>

<sup>a</sup> Institute of Chemistry of New Materials of National Academy of Sciences of Belarus, 220141, Skaryna str, 36, Minsk, Belarus

<sup>b</sup> Åbo Akademi University, Biskopsgatan 8, 20500 Turku/Åbo, Finland

<sup>c</sup> Novosibirsk Institute of Organic Chemistry, Lavrentjev av. 9, 630090, Novosibirsk, Russian Federation

<sup>d</sup> Novosibirsk State University, Pirogova st. 1, 630090, Novosibirsk, Russian Federation

## ARTICLE INFO

### Keywords:

Terpene  
carenes  
Isobenzofuran  
halloysite  
reaction mechanism  
acidity  
DFT

## ABSTRACT

Condensation of a terpene 2-carene with 4-methoxybenzaldehyde over a range of acid aluminosilicates including halloysite nanotubes (HNT) was studied for as a model for preparation of isobenzofuran derivatives with a pharmaceutical potential. The catalysts were characterized by FTIR with pyridine, UV by adsorption of 2-phenylethylamine from the aqueous phase, SEM, TEM and N<sub>2</sub> physisorption. The largest selectivity to the desired product (ca. 70%) over halloysite nanotubes is associated with weak acidity of these catalysts (45 μmol/g), allowing avoiding side isomerization and condensation reactions. Moreover, the highest yield on air-dry HNT clearly indicates that weak Brønsted sites favored the reaction. On the contrary, over strong Brønsted and Lewis acids (Amberlyst-15, scandium triflate), the yield of isobenzofurans did not exceed 16% with formation of mainly 2-carene isomerization products. DFT calculations showed that interactions of the aldehyde with cyclopropane moiety of 2-carene giving isobenzofurans are more beneficial than an alternative direct attack of a proton, leading to side reactions. A possibility to reuse of HNT catalyst was confirmed. Overall, halloysite is a highly effective catalyst for production of isobenzofuran compounds based on 2-carene.

## 1. Introduction

It is well-known that compounds bearing a tetrahydrofuran moiety exhibit diverse biological activity [1,2]. Thus, many derivatives of isobenzofuran (IBF) have anticancer, antiviral, thrombolytic, antidepressant, and other effects, being active ingredients of several drugs [3–9]. In addition, substances with an isobenzofuran structure can be used as part of perfume compositions [10].

The green chemistry principles involve production of chemicals using renewable feedstock [11]. In the context of green chemistry, synthesis of some IBF derivatives was carried out using terpenoids as starting compounds [5,10,12–14]. For example, analogues of the natural compound Sclerophytin A with anticancer activity were obtained from (+)-carvone [5]. Reaction of 4-hydroxymethyl-2-carene with anisaldehyde led to formation of substituted isobenzofurans [12]. In fact, 2-carene *per se*, which is present in small amounts in various essential oils, can be used for synthesis of IBF, if itself it can be obtained

by catalytic isomerization of 3-carene i.e. one of the major components of turpentine [15–17].

Condensation of 2-carene **1** with aldehydes **2** on K-10 clay leads to formation of hexahydroisobenzofurans **3** (as two diastereomers) and compounds with 3-oxabicyclo[3.3.1]nonane structure **4** (Fig. 1a). However, the IBF yield was just below 33% at 75–78% 2-carene conversion [14]. In addition, under acid catalysis conditions carenes can be isomerized (Fig. 1b) with the formation of terpene hydrocarbons **5** with a *p*-menthane structure [14–16].

A study of the biological activity of isobenzofurans synthesized based on 2-carene showed that the product of condensation with vanillin (yield of 33%) demonstrated a pronounced neuroprotective activity in the Parkinson's disease model *in vivo* [18]. Considering the pharmaceutical potential of IBF, development of effective catalytic methods for their synthesis from renewable terpenoids is an important task. Note that a method was recently proposed for isobenzofurans preparation based on a mixture of vanillin and 2-carene, where the

\* Corresponding author at: Institute of Chemistry of New Materials of National Academy of Sciences of Belarus, 220141, Skaryna str, 36, Minsk, Belarus.

\*\* Corresponding author at: Åbo Akademi University, Biskopsgatan 8, 20500, Turku/Åbo, Finland.

E-mail addresses: [Sidorenko@ichnm.basnet.by](mailto:Sidorenko@ichnm.basnet.by) (A.Y. Sidorenko), [dmurzin@abo.fi](mailto:dmurzin@abo.fi) (D.Y. Murzin).

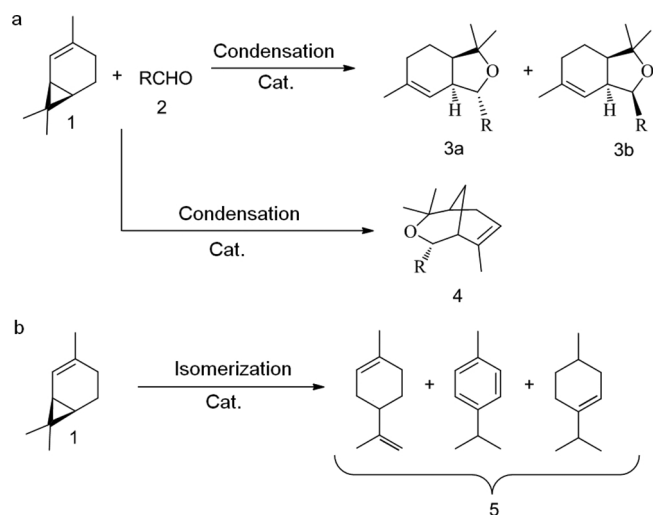


Fig. 1. Scheme of 2-carene condensation with aldehydes (a) and isomerization (b) in the presence of acid catalysts.

latter was obtained by 3-carene isomerization [19]. However, condensation of 2-carene *per se* with aldehydes over various catalysts has not been systematically studied.

Halloysite is a natural aluminosilicate (clay mineral), the elementary layer of which is a combination of tetrahedral Si–O and octahedral Al–O sheets [20–21]. Morphologically, this mineral is a nanoscale multilayer tubes (Fig. S1, Supplementary Information). Halloysite nanotubes (HNT) can be used as containers for controlled release of various agents, as adsorbents for industrial pollutants, as a part of biocomposites, etc. [21–23]. Much less common is application of HNT as acid catalysts [24–26].

Recently, it was shown that acid-modified halloysite is an active, selective, and stable catalyst for the synthesis of physiologically active chromene compounds based on terpenoid (-)-isopulegol [27,28]. Accordingly, halloysite can have a significant potential as a catalyst for preparation of isobenzofurans based on 2-carene.

In the present work, condensation of 2-carene 1 with anisaldehyde (4-methoxybenzaldehyde) 2 was used as a model reaction for preparation of isobenzofuran derivatives preparation. The choice of the reactant 4-methoxybenzaldehyde was based on its higher reactivity compared to vanillin whereas a parent arylaldehyde (i.e. benzaldehyde) does not react with 2-carene [14]. 2-Carene containing mixture obtained by 3-carene isomerization was also tested as starting material.

## 2. Experimental

### 2.1. Preparation and characterization of the catalysts

The starting material for the catalyst preparation was halloysite from the Dragon Mine (USA). Commercial montmorillonite clays K-10, K-30 (Germany), illite clay (Russia), as well as strong Brønsted (Amberlyst-15) and Lewis (scandium triflate) acids were used for comparison. All commercially available materials including halloysite were purchased from Sigma-Aldrich. The reference illite sample was kindly provided by the Belarusian Scientific Research Geological Exploration Institute. Its physicochemical characteristics were carefully studied in [27].

The acid treatment of HNT was carried out using the following procedure [27]. First 5–7 g of solid were added to a three-necked flask (50 ml) equipped with a reflux condenser and a thermometer, and then 5% HCl solution was added at the rate of 5 ml of solution per 1 g of clay. The mixture was heated to 90 °C and stirred (300 rpm) at this temperature for 3 h. Thereafter, halloysite was washed by decantation until there were no Cl<sup>-</sup> ions (control with AgNO<sub>3</sub>). The solid phase was dried

at 105 °C to a constant weight, grinded to a fine powder and held for at least 72 h to obtain an air-dry state of the catalyst. Illite was activated similarly using 10% HCl. For all studies, a catalyst fraction of less than 100 μm was used.

Halloysite nanotubes modified by hydrochloric acid with different concentrations were previously characterized by XRD, XRF, MAS NMR, SEM, TEM, SAED, FTIR with pyridine and N<sub>2</sub> physisorption methods [27,28]. In the current work, the following methods were applied to analyze the studied materials.

A JEOL JEM-2100 transmission electron microscope was used to obtain images of halloysite. The samples were prepared by applying an aqueous dispersion to a copper plate, followed by drying. Photographs of scanning electron microscopy (SEM) were obtained on a Zeiss Leo 1530 microscope after preliminary ultrasonic treatment with HNT.

The porous structure of aluminosilicates was studied with N<sub>2</sub> physisorption using ASAP 2020 MP (Micromeritics) analyzer. The samples (ca. 50 mg) were evacuated (residual pressure 0.013 Pa) for 1 h at 200 °C. The specific surface area was calculated by the Brunauer-Emmett-Teller method. The volume and average pore diameter were determined by the desorption branch of the isotherm using the Barrett-Joyner-Halenda method [29].

The acidity of the studied solids was determined by FTIR spectroscopy using pyridine as a probe molecule [30]. The samples were preliminarily calcined at 350 °C for 1 h, then cooled to 100 °C and pyridine was saturated at this temperature for 30 min. Identification of Brønsted and Lewis acid sites (a.s) was carried out by absorption bands at 1545 cm<sup>-1</sup> and 1450 cm<sup>-1</sup> respectively [31]. The concentration of weak, medium, and strong a.s. was determined by the peak areas at 150 °C, medium and strong at 250 °C, while strong sites correspond to desorption at 350 °C [32].

In addition, acidity HNT, K-10, K-30, and IL materials were determined by adsorption of 2-phenylethylamine from aqueous solutions [33]. For such measurements 3.0 ml of an amine aqueous solution (0.03 M) was added to ca. 50 mg of the catalyst dried at 110 °C and stirred at room temperature for 2 h. After the catalyst separation, the amine content in the filtrate was analyzed by UV spectroscopy (Shimadzu UV-2550) at a wavelength of 252 nm. The concentration of a.s. corresponded to the amount of adsorbed 2-phenylethylamine.

### 2.2. Reaction and analysis of products

All reagents were purchased from Sigma-Aldrich and had a purity of at least 97%. The reaction of 2-carene 1 with 4-methoxybenzaldehyde 2 was carried out according to the following procedure. Substrate 1 (0.1 g), an equivalent amount of aldehyde, 0.1 g of tridecane (99.9%, internal standard) and dried cyclohexane as a solvent were added to a three-necked round bottom flask. The total volume of the mixture was 5.0 ml. After heating to 50 °C, 1.0 g of catalyst was added to the flask and stirred at this temperature using a mechanical stirrer (600 rpm). An excess of the catalyst was needed to have feasible reactivity. Samples of the reaction mixture periodically taken from the reactor after addition of ethyl acetate, vigorous shaking, and catalyst separation were analyzed by GC. The reaction in the presence of scandium triflate (30 mol. %) as a homogeneous catalyst was carried out at 40 °C using methylene chloride (5 ml) as a solvent.

The composition of the reaction mixture was determined using a Khromos GKh-1000 gas chromatograph with a flame ionization detector, a Zebron ZB-5 capillary column (30 m x 0.25 mm x 0.25 μm), and helium as a carrier gas. The evaporator and detector temperature was 250 °C and 280 °C respectively. The temperature increase was realized from 50 to 280 °C at a ramping rate of 15 °C/min followed by an isothermal mode at 280 °C. The total analysis time was 25 minutes. A typical chromatogram of the reaction mixture is shown in Fig. S2.

The reaction mixture was separated by preparative column chromatography. The structure of the reaction products was determined using <sup>1</sup>H and <sup>13</sup>C NMR spectroscopy and a high resolution mass

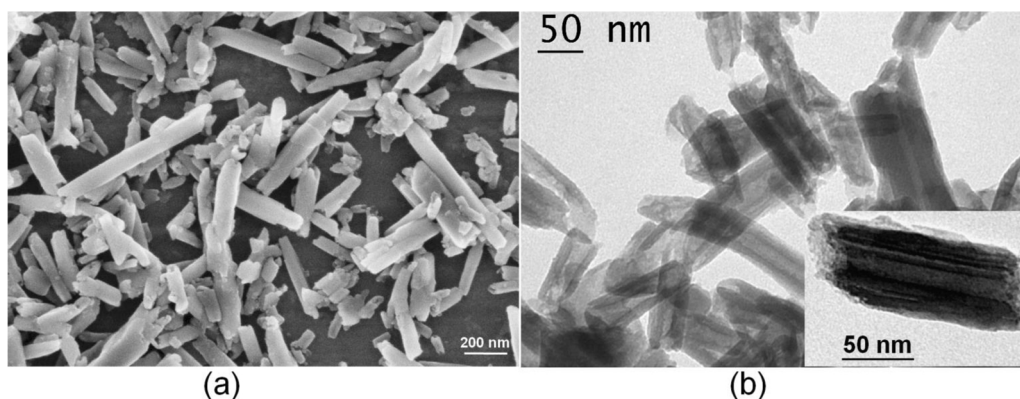


Fig. 2. Images of scanning (a) and transmission (b) electron microscopy of treated with 5% HCl halloysite nanotubes.

spectrometry. Detailed procedures for isolating and verification of the compounds structure are presented in Supplementary Information.

### 3. Results and Discussion

#### 3.1. Catalyst morphology and properties

Images of scanning and transmission electron microscopy of the acid-treated halloysite demonstrate characteristic multilayer nanoscale tubes (Fig. 2). Destruction sites were observed at the ends of HNT (Fig. 2b), which is associated with the rupture of Si–O–Al bonds between the tetra- and octahedral halloysite sheets as a result of acid action and subsequent crosslinking of Si–OH fragments with the formation of amorphous SiO<sub>2</sub> [27,34]. Note that modification of HNT with 5% HCl led to a slight decrease in the Al<sub>2</sub>O<sub>3</sub> content while their specific surface area increased from 60 to 130 m<sup>2</sup>/g (Table S1). All the studied aluminosilicates are mesoporous (Table S1). Adsorption-desorption isotherms were shown in the previous work of the authors [27].

According to FTIR spectroscopy with pyridine, concentration of a.s. in halloysite nanotubes increased from 34 to 45 μmol/g after their treatment with 5% HCl. At the same time, weak acid sites prevail in HNT (Table S2). Montmorillonites K-10 and K-30, as well as acid-activated illite IL were more acidic. It is important to note that acidity according to FTIR correlates well with the values obtained by the adsorption of 2-phenylethylamine from an aqueous solution (Fig. 3).

Although the concentration of a.s. measured using pyridine was significantly lower probably due to the catalyst pretreatment at 350 °C, a linear correlation between the values obtained by different methods clearly demonstrates relevance of using FTIR for characterization of

catalysts applied in low-temperature reactions.

#### 3.2. Catalytic activity of studied catalysts

##### 3.2.1. Products selectivity and mechanistic discussion

In the presence of initial HNT, the condensation of 2-carene **1** with 4-methoxybenzaldehyde **2** practically did not proceed. Over acid-treated halloysite, selectivity to isobenzofurans **3** (70.9%) was significantly higher compared with montmorillonites K-10, K-30 and illite IL (Table 1). The diastereomers ratio **3a/3b** on HNT was lower than for K-10 and K-30 catalysts. Formation of a small amount (0.8%) of compounds with 3-oxabicyclo[3.3.1]nonane structure **4** was observed on halloysite, whereas 2-carene isomerization products **5** were absent. The largest initial 2-carene consumption rate ( $r_0$ ) was observed on K-10 and K-30 (Table 1).

On the other hand, over strong Brønsted (Amberlyst-15) and Lewis (scandium triflate) acids 2-carene predominantly isomerized into terpene hydrocarbons **5** (menthadienes, cymenes, menthenes), giving accordingly very low selectivity to IBF **3** (Table 1).

Selectivity to isobenzofuran **3** in the presence of halloysite decreases with increasing 2-carene conversion (Fig. 4a,b). In this case, an increase in the ratio **3a/3b** was observed (Fig. 4c). These dependences may indicate further transformations of isobenzofurans under reaction conditions. Indeed, storage of a diastereomers **3a,b** mixture on K-10 clay led to a decrease in their amount, moreover the GC peak intensity of the isomer **3b** decreased to a larger extent (Fig. S3).

Based on the dependences of selectivity to isobenzofurans **3** on 2-carene conversion (Fig. 4), as well as the results of their storage on K-10 (Fig. S3), it can be concluded that compounds **3** in the reaction conditions undergo secondary transformations (apparently polymerization), the isomer **3b** being less stable. The largest concentration of isobenzofurans **3** in the reaction mixture was observed at 60% 2-carene

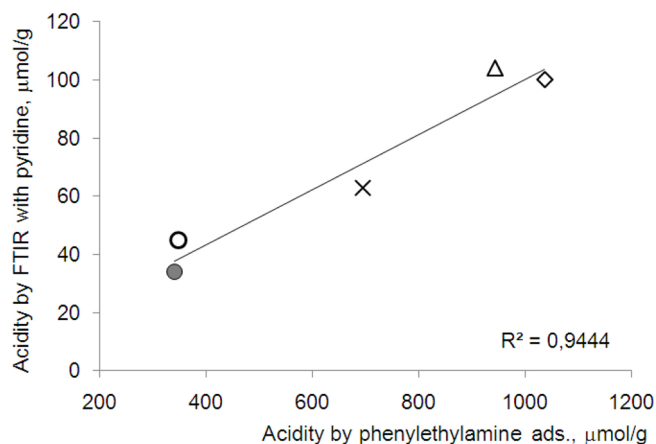


Fig. 3. Dependence of acidity measured by FTIR with pyridine adsorption and 2-phenyl 2-phenylethylamine adsorption from the liquid phase.

(●–Initial and ○ – acid-modified halloysite; X – IL; Δ – K-10; ◇ – K-30)

Table 1  
Selectivity<sup>a</sup> in 2-carene condensation with anisaldehyde over studied catalysts.

| Catalyst <sup>b</sup>             | $r_0^c$ ,<br>μmol/<br>(g·min) | Reaction<br>time, h | Selectivity, mol. % |      |      |       |      |      |
|-----------------------------------|-------------------------------|---------------------|---------------------|------|------|-------|------|------|
|                                   |                               |                     | 3                   | 3a   | 3b   | 3a/3b | 4    | 5    |
| HNT                               | 8.6                           | 2                   | 70.9                | 49.7 | 21.2 | 2.3   | 0.8  | 0    |
| IL                                | 4.2                           | 4                   | 50.3                | 32.8 | 17.5 | 1.9   | 1.9  | 1.3  |
| K-30                              | 14.3                          | 3                   | 51.4                | 40.7 | 10.7 | 3.8   | 2.7  | 3.8  |
| K-10                              | 14.4                          | 3                   | 52.3                | 43.8 | 8.5  | 5.2   | 2.2  | 5.1  |
| Amberlyst-15                      | 7.6                           | 2                   | 3.0                 | 2.4  | 0.6  | 4.0   | 12.9 | 52.3 |
| Scandium<br>triflate <sup>d</sup> | -                             | 3                   | 16.3                | 12.2 | 4.1  | 3.0   | 6.4  | 77.0 |

<sup>a</sup> At 60% 2-carene conversion.

<sup>b</sup> Air-dry state.

<sup>c</sup> Initial rate of 2-carene consumption.

<sup>d</sup> At 20% conversion.

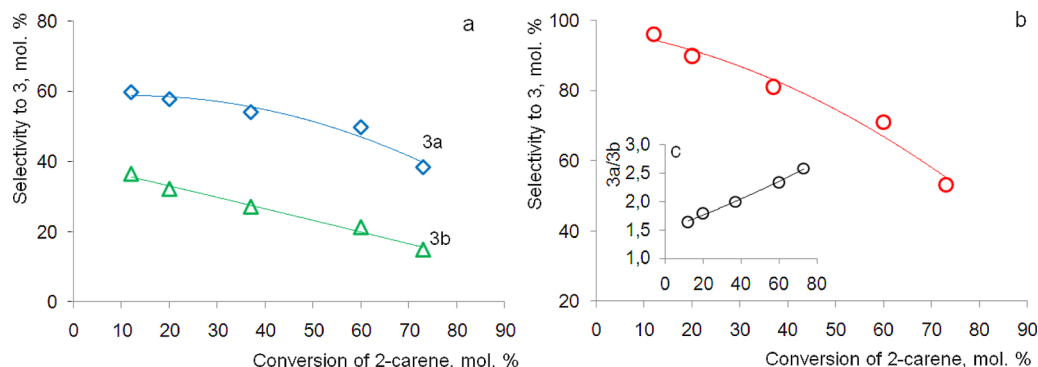


Fig. 4. Selectivity to isobenzofuran isomers (a), their sum (b) and **3a/3b** ratio (c) as a function of 2-carene conversion over halloysite.

conversion (Fig. S4). Note that although the initial rate of 2-carene consumption on K-10 is much higher than for HNT, 60% conversion was observed only after 3 h (Table 1). The form of concentration dependencies clearly indicates K-10 catalyst deactivation (Fig. S5), probably due to formation of polymerization products.

When the reaction mixture obtained on HNT after complete conversion of 2-carene was separated, isobenzofurans **3** (34%) and two products with 3-oxabicyclo[3.3.1]nonane structure **4** (2 %) were isolated, one of which had a diene moiety (Supplementary Information).

To understand the reasons of different selectivity over studied materials, an analysis of the isobenzofurans yield dependence on catalysts acidity was carried out.

Selectivity towards isobenzofurans **3** decreases from 70.9 to 50.2% with an increase in the a.s. concentration in the catalyst from 45 to 63  $\mu\text{mol/g}$  and remains almost unchanged with a further increase in acidity (Fig. 5a). At the same time the isomers **3a/3b** ratio increases (Fig. 5b). This dependence can be explained by a lower stability of compound **3b** under the reaction conditions compared with **3a**. Thus, **3b** over more acidic catalysts K-10 and K-30 undergoes secondary transformations. It is also important to note that with an increase in the ratio of weak (W) to the sum of medium (M) and strong (S) acid sites, a significant increase in IBF selectivity was observed (Fig. 5c).

Based on the discussion above, the highest selectivity to isobenzofurans **3** in the presence of halloysite is due to low acidity of this catalyst. Moreover, a decrease in IBF selectivity with an increase in the a.s. concentration is due to secondary transformations (polymerization) of the compound **3** under the reaction conditions, especially **3b**. It is important to note that the isomerization by-products **5** and compounds with 3-oxabicyclo[3.3.1]nonane structure **4** on all studied aluminosilicate catalysts (halloysite, illite, montmorillonites) are formed in very small quantities (Table 1).

Similar results were observed in the case of terpene  $\beta$ -pinene condensation with paraformaldehyde to nopol, where selective formation of this product occurred on weak Lewis and Brønsted a.s, while the

strong Brønsted acidity caused  $\beta$ -pinene isomerization [35]. Moreover, heteropolyacids (HPW/SiO<sub>2</sub>) catalyzed the  $\beta$ -pinene condensation with aldehydes to oxabicyclo[3.3.1]nonane compounds [36].

Thus, on aluminosilicates with a relatively low acidity, condensation of 2-carene **1** with 4-methoxybenzaldehyde **2** occurs with the involvement of the cyclopropane ring, leading to formation of isobenzofuran **3** as two diastereomers depending on the chiral carbon atom configuration in the intermediates (Fig. 6). In the presence of strong Brønsted (Amberlyst-15) and Lewis (scandium triflate) acids, the cyclopropane moiety in 2-carene is opened with formation of an intermediate **1'** with a *p*-menthane structure, which in a subsequent reaction with the aldehyde gives 3-oxabicyclo[3.3.1]nonane compound **4** (Fig. 6). However, considering that terpene hydrocarbons **5** are the main products on Amberlyst-15 and scandium triflate (Table 1), it can be assumed that, in the presence of strong acids, ion **1'** is predominantly deprotonated to form isomerization products.

### 3.2.2. Influence of halloysite thermal pretreatment

Taking into account that selectivity of the reactions of terpenoids can strongly depend on the catalyst thermal treatment conditions [27,32], the reaction of 2-carene with anisaldehyde was studied in the presence of acid-modified halloysite, dried at temperatures from 50 to 105 °C for 2 h immediately before the reaction.

After HNT thermal pretreatment at 50 °C, selectivity to isobenzofurans **3** (73.7%) was slightly higher compared with an air-dried one (70.9%), however, the initial rate of 2-carene consumption increased (Table 2). A further increase in the catalyst drying temperature led to a sharp decrease in IBF yield, whereas compounds with 3-oxabicyclo[3.3.1]nonane structure **4** and products of 2-carene isomerization **5** were dominant in the reaction mixture (Table 2).

Note that the time to reach 60% conversion on halloysite nanotubes dried at 60 – 105 °C was longer than for air-dried HNT (Table 2). This can be explained by a partial deactivation of the catalyst, which is indicated by the characteristic kinetic curves (Fig. S6), as well as a change

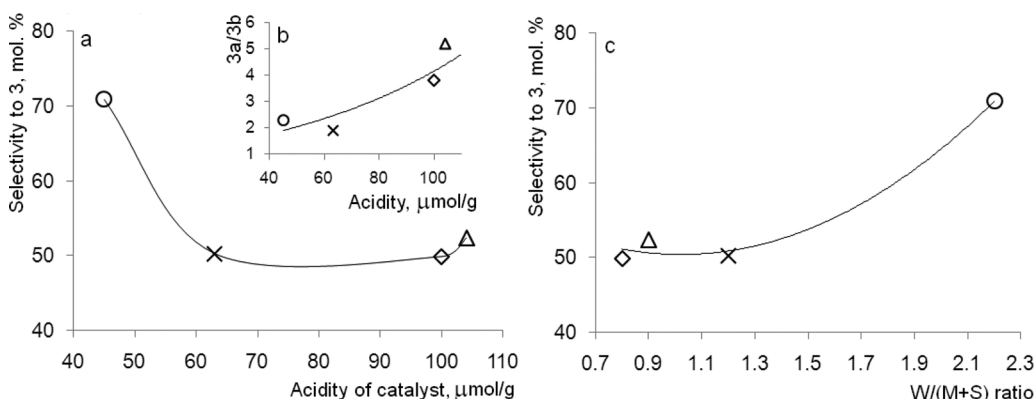


Fig. 5. Selectivity to isobenzofuran (a) and **3a/3b** ratio (b) as a function of catalyst acidity as well as a ratio of weak to sum of medium and strong a.s. (c) at 60% 2-carene conversion. (○ – Acid-modified halloysite; X – IL;  $\Delta$  – K-10;  $\diamond$  – K-30).

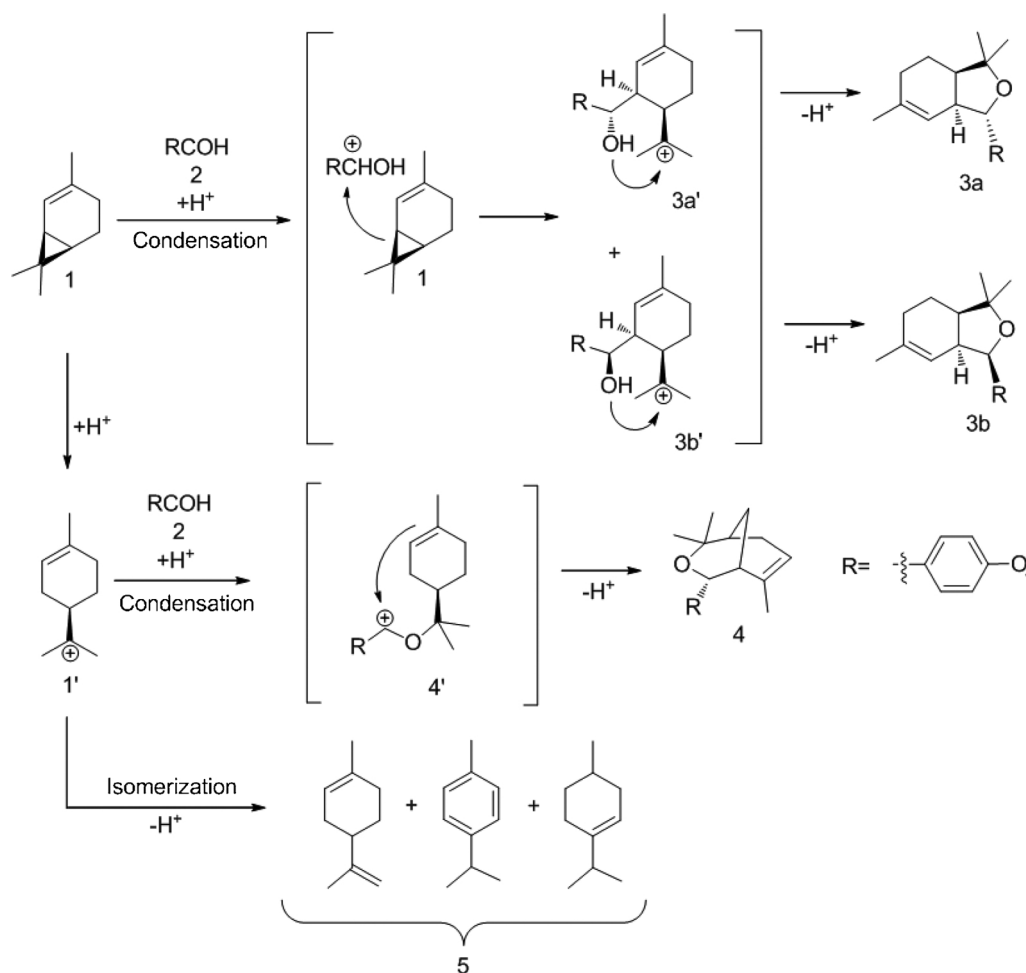


Fig. 6. The mechanism of 2-carene condensation with aldehydes.

Table 2

Selectivity of 2-carene<sup>a</sup> reaction with anisaldehyde depending on the HNT drying temperature.

| Temperature of HNT drying, °C | $r_o$ , $\mu\text{mol}/(\text{g}\cdot\text{min})$ | Reaction time, h | Selectivity, mol. % |      |      |       |      |      |
|-------------------------------|---|------------------|---------------------|------|------|-------|------|------|
|                               |   |                  | 3                   | 3a   | 3b   | 3a/3b | 4    | 5    |
| Air-dry                       | 8.6   | 2                | 70.9                | 49.7 | 21.2 | 2.3   | 0.8  | -    |
| 50                            | 26.1  | 0.5              | 73.7                | 54.4 | 19.3 | 2.8   | 0.9  | 2.5  |
| 60                            | 7.2   | 4                | 13.3                | 10.0 | 3.2  | 3.1   | 23.2 | 23.7 |
| 70                            | 7.9   | 4                | 11.6                | 8.5  | 3.2  | 2.7   | 36.9 | 22.3 |
| 105                           | 8.4   | 5                | 7.3                 | 6.4  | 0.9  | 6.8   | 27.2 | 33.3 |

<sup>a</sup> At 60% conversion.

in the color of the reaction mixture (Fig. S7) due to formation of secondary products.

A sharp decrease in the isobenzofurans yield with an increase in the halloysite drying temperature can be explained by a change in the nature and strength of active sites on the catalyst surface. Thus, acidity of layered silicates (including halloysite) is associated with exchange and coordinatively unsaturated metal ions, hydroxyl groups, water molecules bound to cations [37]. Water molecules due to interactions with the metal cations (Lewis a.s.) are polarized and act as Brønsted acids according to the scheme  $[\text{L}(\text{H}_2\text{O})_x]^{2+} = [\text{L}(\text{OH})(\text{H}_2\text{O})_{x-1}]^{2+} + \text{H}^+$ . It is known that with increasing hydration of the aluminosilicate surface, the strength of such acid sites is decreasing [37].

Drying of halloysite led to its dehydration (Table S3) and a sharp decrease in the yield of isobenzofurans **3**, i.e. these compounds are selectively formed when weak Brønsted acidity prevails. This is

consistent with data on the effect of catalyst acidity on the yield of these compounds (Fig. 5). An increase in the strength of a.s. due to dehydration of halloysite (drying at 60–105 °C) leads to occurrence of the side reactions of 2-carene isomerization as well as formation of compounds with 3-oxabicyclo[3.3.1]nonane structure (Table 2).

### 3.2.3. DFT calculations

To further evaluate the proposed mechanism for 2-carene condensation with 4-methoxybenzaldehyde (Fig. 6), DFT calculations performed with the Jaguar 9.9 program [38] using dispersion-corrected hybrid density functional technique B3LYP-D3 implanted with a 6-31G\*\* basis set for structural geometry optimization.

The calculated energies for intermediates **3a'** and **3b'** generated during interactions of the aldehyde with the cyclopropane ring of 2-carene were significantly lower than in the alternative path, where 2-carene was converted into *p*-menthenyl cation **1'** (Fig. 7). The energy for the intermediate **3a'** was 6.0 kJ/mol lower than for **3b'**, and the resulting diastereomer **3a** was 6.8 kJ/mol more stable compared to **3b**. Note that the DFT optimization of the intermediates **3a'**, **b'** structure showed that their isopropyl fragment with a charge on carbon is not planar (Fig. 7), which obviously facilitates further cyclization into isobenzofurans **3a**, **b**. The optimized structures of substrate **1**, as well as the reaction products **3a**, **b** and **4** are shown in Fig. S8

Thus, DFT calculations show that formation of isobenzofurans with the participation of the cyclopropane fragment of 2-carene is thermodynamically more favorable than formation of *p*-menthenyl ion leading to the 3-oxabicyclo[3.3.1]nonane compound. The predominant production of diastereomer **3a** is energetically more favorable compared



**Table 5**  
Physico-chemical properties of halloysite nanotubes after utilization in the reaction

| Halloysite           | Porous structure                         |   |                         | Acid site concentration, $\mu\text{mol/g}$ |
|----------------------|--|---|-------------------------|--|
|                      | $S_{\text{BET}}$ , $\text{m}^2/\text{g}$ | $V_{\text{pores}}$ , $\text{cm}^3/\text{g}$ | $D_{\text{pores}}$ , nm |  |
| Fresh                | 129                                      | 0.34  | 11.3                    | 45.0                                       |
| After reaction cycle | 114                                      | 0.36  | 13.9                    | 43.0                                       |

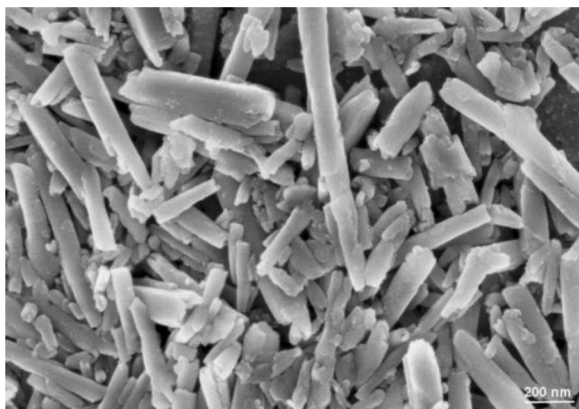


**Fig. 8.** SEM image of halloysite nanotubes after utilization in the reaction.

the specific surface area was observed, while the concentration of acid sites remained practically unchanged (Table 5). According to scanning electron microscopy, the morphology of halloysite particles after the reaction did not change either (Fig. 8).

#### 4. Conclusions

Condensation of the natural terpene 2-carene with 4-methoxybenzaldehyde on a range of acid aluminosilicate (halloysite nanotubes, illite, montmorillonites K-10, K-30) was studied for the first time as a model for preparation of isobenzofuran derivatives with a pharmaceutical potential. Strong Brønsted (Amberlyst-15) and Lewis (scandium triflate) acids were used as reference catalysts.

Selectivity towards isobenzofurans over studied aluminosilicates increases from 52 to 71% with a decrease in the acid sites concentration from 104 to 45  $\mu\text{mol/g}$ , respectively. On strong Brønsted and Lewis acids, the yield of isobenzofurans did not exceed 16%, whereas a predominant formation of the 2-carene isomerization products and compounds with 3-oxabicyclo[3.3.1]nonane structure was observed.

Therefore, the largest selectivity to isobenzofurans in the presence of halloysite nanotubes is associated with weak acidity of these catalysts, allowing avoiding side reactions of isomerization and condensation. The isobenzofuran yield sharply decreased with an increase in the drying temperature of halloysite, which clearly indicates its formation on weak Brønsted acid sites.

According to DFT calculations, the involvement of cyclopropane moiety of 2-carene in the condensation with anisaldehyde leading to isobenzofurans formation, was energetically preferable compared to 2-carene transformations to *p*-menthenyl ion, giving side products. The predominant formation of one of the possible diastereoisomers was also due to thermodynamic reasons.

Considering that 2-carene is an expensive compound, a possibility of halloysite utilization for isobenzofurans synthesis was demonstrated using a 2-carene containing mixture obtained by isomerization of cheap 3-carene. Moreover, a possibility to reuse halloysite nanotubes without catalytic activity decrease was confirmed.

Thus, halloysite is a highly effective catalyst for production of

isobenzofuran compounds with a pharmaceutical potential based on terpene 2-carene. Further research should be directed to the catalytic synthesis of other isobenzofuran derivatives and elucidation their physiological activity.

#### CRedit authorship contribution statement

**A.Yu. Sidorenko:** Conceptualization, Investigation, Writing - original draft. **A.V. Kravtsova:** Investigation, Methodology. **P. Mäki-Arvela:** Methodology, Investigation. **A. Aho:** Investigation. **T. Sandberg:** Formal analysis. **I.V. Il'ina:** Investigation. **N.S. Li-Zhulanov:** Formal analysis. **D.V. Korchagina:** Investigation. **K.P. Volcho:** Writing - review & editing. **N.F. Salakhutdinov:** Writing - review & editing. **D.Yu. Murzin:** Writing - review & editing, Supervising. **V.E. Agabekov:** Writing - review & editing, Project administration.

#### Declaration of Competing Interest

The authors declare no conflict of interest.

#### Acknowledgments

This work was funded by the BRFFR (grant Kh18MS-029) and RFBR (grant 19-53-04005). The research visit of A.S. to ÅAU to study physico-chemical properties of the catalysts was financially supported by Research Mobility Program of Åbo Akademi University. The authors are grateful to Dr. T.F. Kuznetsova (IGCh of NAS of Belarus) for performing  $\text{N}_2$  physisorption and to Dr. H. Pazniak for recording TEM images.

#### Appendix A. Supplementary data

Supplementary material related to this article can be found, in the online version, at doi:<https://doi.org/10.1016/j.mcat.2020.110974>.

#### References

- [1] C.M. Marson, *Adv. Heterocycl. Chem* 121 (2017) 13–33.
- [2] Q. Lu, D.S. Harmalkar, Y. Choi, K. Lee, An overview of saturated cyclic ethers: Biological profiles and synthetic strategies, *Molecules* 24 (2019) 3778.
- [3] J.F.M. Hewitt, L. Williams, P. Aggarwal, C.D. Smith, D.J. France, Palladium-catalyzed heteroallylation of unactivated alkenes – synthesis of citalopram, *Chem. Sci* 4 (2013) 3538–3543.
- [4] S. Joardar, S. Chakravorty, S.P. Das, A simple, convenient, highly regioselective synthesis of isobenzofuran-1(3H)-ones (phthalides) as well as Maculalactone A & B, the bioactive butyrolactones, *Lett. Org. Chem* 13 (2016) 127–134.
- [5] D. Bateman, A.L. Joshi, K. Moon, E.N. Galitovskaya, M. Upreti, T.C. Chambers, M.C. McIntosh, Synthesis and anticancer activity of sclerophytin-inspired hydro-isobenzofurans, *Bioorg. Med. Chem. Lett.* 19 (2009) 6898–6901.
- [6] P. He, P. Yang, Ye L.S.Tang, C. Liu, Q. Shen, D. Tang, F. Zhang, Z. Liu, Y. Chen, S. Yao, N. Xiang, Z. Huang, Three new isobenzofurans from the roots of *Nicotiana glauca* and their bioactivities, *Nat. Prod. Res.* 23 (2017) 2730–2736.
- [7] S. Zhang, H. Zhang, S. Yang, C. Qu, Z. Xie, G. Pescitelli, Isolation, stereochemical study, and cytotoxic activity of isobenzofuran derivatives from a marine streptomyces sp, *Chirality* 27 (2015) 82–87.
- [8] A.S. de Oliveira, P.A.R. Gazolla, A.F.C. da S. Oliveira, W.L. Pereira, L.C. de S. Viol, A.F. da S. Maia, E.G. Santos, Í.E.P. da Silva, T.A. de Oliveira Mendes, A.M. da Silva, R.S. Dias, C.C. da Silva, M.D. Polêto, R.R. Teixeira, S.O. de Paula, Discovery of novel West Nile Virus protease inhibitor based on isobenzofuranone and triazolic derivatives of eugenol and indan-1,3-dione scaffolds, *PLoS ONE* 14 (2019) e0223017.
- [9] F. Ma, Y. Gao, H. Qiao, X. Hu, J. Chang, Antiplatelet activity of 3-butyl-6-bromo-1(3H)-isobenzofuranone on rat platelet aggregation, *J. Thromb. Thrombolysis* 33 (2012) 64–73.
- [10] S. Wahidullah, M.B. Govenkar, S.K. Paknikar, US7138368B2, 2003.
- [11] R.A. Sheldon, Green and sustainable manufacture of chemicals from biomass: state of the art, *Green Chem* 16 (2014) 950–963.
- [12] B. Maurer, A. Hauser, G. Ohloff, New sesquiterpenoids from cabreuva oil, *Helv. Chim. Acta* 69 (1986) 2026–2037.
- [13] S.Yu. Kurbakova, I.V. Il'ina, O.S. Mikhailchenko, M.A. Pokrovsky, D.V. Korchagina, K.P. Volcho, A.G. Pokrovsky, N.F. Salakhutdinov, The short way to chiral compounds with hexahydrofluorenol[9,1-bc]furan framework: Synthesis and cytotoxic activity, *Bioorg. Med. Chem.* 23 (2015) 1472–1480.
- [14] I.V. Il'ina, K.P. Volcho, D.V. Korchagina, G.E. Salnikov, A.M. Genaeu, E.V. Karpova, N.F. Salakhutdinov, Unusual reactions of (+)-car-2-ene and (+)-car-3-ene with

- aldehydes on K10 clay, *Helv. Chim. Acta* 93 (2010) 2135–2150.
- [15] A.Yu. Sidorenko, A. Aho, J. Ganbaatar, D. Batsuren, D.B. Utenkova, G.M. Sen'kov, J. Wärnä, D.Yu. Murzin, V.E. Agabekov, Catalytic isomerization of  $\alpha$ -pinene and 3-carene in the presence of modified layered aluminosilicates, *Mol. Catal.* 443 (2017) 193–202.
- [16] D.B. Utenkova, E.D. Skakovskii, G.M. Senkov, A.V. Baranovskii, S.E. Bogushevich, A. Yu. Sidorenko, NMR and GC Analyses of 3-Carene isomerization products over activated glauconite, *J. Appl. Spect.* 83 (2017) 1026–1030.
- [17] U. Meyer, W.F. Hoelderich, Application of basic zeolites in the decomposition reaction of 2-methyl-3-butyn-2-ol and the isomerization of 3-carene, *J. Mol. Catal. A: Chem* 142 (1999) 213–222.
- [18] A.V. Pavlova, I.V. Il'ina, E.A. Morozova, D.V. Korchagina, S.Yu. Kurbakova, I.V. Sorokina, T.G. Tolstikova, K.P. Volcho, N.F. Salakhutdinov, Potent neuroprotective activity of monoterpene derived 4-[(3aR,7aS)-1,3,3a, 4,5,7a-hexahydro-3,3,6-trimethylisobenzofuran-1-yl]-2-methoxyphenol in MPTP mice model, *Lett. Drug Design Discov* 11 (2014) 611–617.
- [19] A.Yu. Sidorenko, I.V. Il'ina, A.V. Kravtsova, A. Aho, O.V. Ardashov, N.S. Li-Zhulanov, K.P. Volcho, N.F. Salakhutdinov, D.Yu. Murzin, V.E. Agabekov, Preparation of chiral isobenzofurans from 3-carene in the presence of modified clays, *Mol. Catal.* 459 (2018) 38–45.
- [20] E. Joussein, S. Petit, J. Churchman, B. Theng, D. Righi, B. Delvaux, Halloysite clay mineral – a review, *Clay Min.* 40 (2005) 383–426.
- [21] P. Yuan, D. Tan, F. Annabi-Bergaya, Properties and applications of halloysite nanotubes: recent research advances and future prospects, *Appl. Clay. Sci.* 112–113 (2015) 75–93.
- [22] Y. Lvov, A. Aerov, R. Fakhru'llin, Clay nanotube encapsulation for functional biocomposites, *Adv. Colloid Interface Sci.* 207 (2014) 189–198.
- [23] M. Tharmavaram, G. Pandey, D. Rawtani, Surface modified halloysite nanotubes: A flexible interface for biological, environmental and catalytic applications, *Adv. Colloid Interf. Sci.* 261 (2018) 82–101.
- [24] V.M. Abbasov, H.C. Ibrahimov, G.S. Mukhtarova, E. Abdullayev, Acid treated halloysite clay nanotubes as catalyst supports for fuel production by catalytic hydrocracking of heavy crude oil, *Fuel* 184 (2016) 555–558.
- [25] S.M. Silva, A.F. Peixoto, C. Freire, HSO<sub>3</sub>-functionalized halloysite nanotubes: New acid catalysts for esterification of free fatty acid mixture as hybrid feedstock model for biodiesel production, *Appl. Catal. A: Gen.* 568 (2018) 221–230.
- [26] A.A. Krasilin, E.A. Straumal, L.L. Yurkova, E.K. Khrapova, M.V. Tomkovich, I.G. Shunina, L.P. Vasil'eva, S.A. Lermontov, V.K. Ivanov, Sulfated halloysite nanoscrolls as superacid catalysts for oligomerization of hexene-1, *Rus. J. Appl. Chem* 92 (2019) 1251–1257.
- [27] A.Yu. Sidorenko, A.V. Kravtsova, A. Aho, I. Heinmaa, J. Warna, H. Pazniak, K.P. Volcho, N.F. Salakhutdinov, D.Yu. Murzin, V.E. Agabekov, Highly selective Prins reaction over acid-modified halloysite nanotubes for synthesis of isopulegol-derived 2H-chromene compounds, *J. Catal* 374 (2019) 360–377.
- [28] A.Yu. Sidorenko, A.V. Kravtsova, I.V. Il'ina, J. Wärnä, D.V. Korchagina, Yu.V. Gatilov, K.P. Volcho, N.F. Salakhutdinov, D.Yu. Murzin, V.E. Agabekov, Clay nanotubes catalyzed solvent-free synthesis of octahydro-2H-chromenols with pharmaceutical potential from (-)-isopulegol and ketones, *J. Catal.* 380 (2019) 145–152.
- [29] E.P. Barrett, L.G. Joyner, P.P. Halenda, The determination of pore volume and area distributions in porous substances, *J. Am. Chem. Soc.* 73 (1951) 373–380.
- [30] A. Aho, N. Kumar, K. Eränen, T. Salmi, M. Hupa, D.Yu. Murzin, Catalytic pyrolysis of woody biomass in a fluidized bed reactor: Influence of the zeolite structure, *Fuel* 87 (2008) 2493–2501.
- [31] C.A. Emeis, Determination of Integrated Molar Extinction Coefficients for Infrared Absorption Bands of Pyridine Adsorbed on Solid Acid Catalysts, *J. Catal.* 141 (1993) 347–354.
- [32] A.Yu. Sidorenko, A.V. Kravtsova, A. Aho, I. Heinmaa, T.F. Kuznetsova, D.Yu. Murzin, V.E. Agabekov, Catalytic isomerization of  $\alpha$ -pinene oxide in the presence of acid-modified clays, *Mol. Catal.* 448 (2018) 18–29.
- [33] V. Rac, V. Rakic, D. Stosic, O. Otman, A. Auroux, Hierarchical ZSM-5, Beta and USY zeolites: Acidity assessment by gas and aqueous phase calorimetry and catalytic activity in fructose dehydration reaction, *Microp. Mesop. Mater* 194 (2014) 126–134.
- [34] E. Abdullayev, A. Joshi, W. Wei, Y. Zhao, Y. Lvov, Enlargement of Halloysite Clay Nanotube Lumen by Selective Etching of Aluminum Oxide, *ACS Nano.* 6 (2012) 7216–7226.
- [35] V.S. Marakatti, D. Mumbaraddi, G.V. Shanbhag, A.B. Halgeri, S.P. Maradur, Molybdenum oxide/ $\gamma$ -alumina: an efficient solid acid catalyst for the synthesis of nopol by Prins reaction, *RSC Adv.* 5 (2015) 93452–93462.
- [36] R.F. Cotta, K.A. da Silva Rocha, E.F. Kozhevnikova, I.V. Kozhevnikov, E.V. Gusevskaya, Coupling of monoterpene alkenes and alcohols with benzaldehyde catalyzed by silica-supported tungstophosphoric heteropoly acid, *Appl. Catal. B: Environ* 217 (2017) 92–99.
- [37] S. Yariv, H. Cross, *Organo-Clay Complexes and Interactions*, Marcel Dekker, New York, 2002.
- [38] Jaguar, Schrödinger, LLC, New York, NY, 2018.